PHYSICAL REVIEW D VOLUME 35, NUMBER 3 1 FEBRUARY 1987

Phenomenology of E_6 electroweak models with two extra Z bosons

V. Barger
Physics Department, University of Wisconsin, Madison, Wisconsin 53706

N. G. Deshpande
Institute of Theoretical Science, University of Oregon, Eugene, Oregon 97403

K. Whisnant
Physics Department, Florida State University, Tallahassee, Florida 32306
(Received 9 October 1986)

We examine the possibilities for two extra Z bosons in E_6 electroweak models, assuming electroweak symmetry breaking occurs via the 27 representation of E_6, as required by superstring theories. We compare scenarios where E_6 is broken to a rank-6 or rank-5 group, and discuss means by which the different models may be distinguished.

I. INTRODUCTION

Recent work on superstring theories[1,2] indicates that the $E_8\times E_8'$ superstring theory in 10 dimensions may yield, after compactification, a four-dimensional E_6 gauge group of the strong and electroweak interactions coupling to $N=1$ supergravity. The E_6 group may then be broken to either a rank-5 or rank-6 subgroup.[3] If E_6 is broken to a rank-5 group, the resulting additional U(1) is uniquely specified. This possibility has been discussed at length in the literature.[4,5] When E_6 is broken to a rank-6 group there are two additional U(1) groups which in principle can lead to two extra Z bosons at the electroweak scale. Special cases when one of these extra Z bosons is accessible to present and planned high-energy experiments have been studied before.[6-14]

In this paper we consider the rank-6 breakdown $E_6\to SO(10)\times U(1)_\psi\to SU(5)\times U(1)_\chi\times U(1)_\psi$, where SU(5) contains the usual $SU(3)_c\times SU(2)_L\times U(1)_Y$. We examine the possibilities for two experimentally accessible extra Z bosons in E_6, assuming that electroweak symmetry breaking occurs via the 27 representation, as required by superstring theories. The allowable models may be classified by the size of the two $SU(2)_L$ singlet scalar vacuum expectation values (VEV's) in the 27, relative to the standard electroweak scale. If both singlet VEV's are large, then both extra Z bosons will have a mass above ~ 400 GeV and they do not mix appreciably with the standard Z. Their interactions with fermions are also somewhat constrained. If only one singlet VEV is large, then one extra Z will be heavy and one will be light and may mix with the standard Z; the particular combination of $U(1)_\chi$ and $U(1)_\psi$ which is lighter is determined uniquely. If neither singlet VEV is large, then all three Z bosons may be of comparable mass and could mix. We will examine in detail the cases in which at least one singlet VEV is large and look at some possibilities in which they are not. We compare the rank-6 scenarios with the special case in which E_6 breaks down to a rank-5 group, and discuss means by which the various models may be distinguished. For at least one large singlet VEV (i.e., at least one high-mass extra Z), the rank-6 scenario is not reducible to the rank-5 case.

The paper is organized as follows. In Sec. II we discuss possible theoretical constraints on the VEV's. In Sec. III we present the mass matrix and Lagrangian. In Sec. IV we discuss the cases outlined above. In Sec. V we examine how the cases may be experimentally distinguished. We summarize our results in Sec. VI. In the Appendix we derive some constraints on the Z-boson masses and mixing.

II. CONSTRAINTS FROM SPECIFIC MODELS

Compactification of $E_8\times E_8'$ on a Calabi-Yau manifold K which is not simply connected, but obtained from a covering $\check{K}$ with a discrete symmetry group G: $K=\check{K}/G$, leads to E_6 broken by the Wilson loop mechanism. This low-energy group can be a rank-5 group depending on whether the discrete group G is Abelian or non-Abelian.[2] The chiral matter multiplets arise from zero modes of the E_8 gauge supermultiplet when compactified. In general there will be some number of 27-dimensional representations and some number δ of the paired subsets of states from the $27+\overline{27}$ representations, which depend on the details of the Wilson-line symmetry breaking.[2,15] The Higgs fields that acquire vacuum expectation values and break the low-energy group further to $SU(3)_c\times U(1)_{em}$ are either the superpartners of the chiral 27 multiplets or arise from $27+\overline{27}$ representations. The transformation properties of the neutral components of the 27 that can acquire VEV's are listed in Table I; an equivalent mass matrix would be obtained from $\overline{27}$ contributions. Note that if $\delta=0$, and Higgs fields arise only from chiral 27 multiplets, we would have to require $v_3=\langle\tilde{\nu}_e\rangle=0$ from lepton-number conservation. We shall, however, be more general in this paper and allow for paired subsets of $27,\overline{27}$ representations with quantum numbers of $\tilde{\nu}_e$ (or $\bar{\tilde{\nu}}_e$) to have a nonvanishing VEV. Thus there are three VEV's with $I_3=\frac{1}{2}$; v_1, v_2, and v_3. In order to break the rank-6 group all the way to $SU(3)_c\times U(1)_{em}$ we must further require two $I_{3L}=0$ VEV's:

TABLE I. Vacuum expectation values and quantum numbers for the neutral scalars in the 27 representation.

VEV	SO(10)	SU(5)	I_{3L}	Q_ψ	Q_χ	Notation of Refs. 5 and 16 for rank-5 model
$\langle\tilde{\nu}_e\rangle=v_3$	16	5*	$\frac{1}{2}$	$(\frac{5}{72})^{1/2}$	$-(\frac{3}{8})^{1/2}$	$\langle\nu\rangle=0$
$\langle\tilde{\nu}_E\rangle=v_2$	10	5*	$\frac{1}{2}$	$-(\frac{5}{18})^{1/2}$	$(\frac{1}{6})^{1/2}$	$\langle\bar{H}\rangle=\bar{v}$
$\langle\tilde{N}_E\rangle=v_1$	10*	5*	$\frac{1}{2}$	$(\frac{5}{18})^{1/2}$	$(\frac{1}{6})^{1/2}$	$\langle H\rangle=v$
$\langle\tilde{N}^c\rangle=\chi_1$	16	1	0	$(\frac{5}{72})^{1/2}$	$(\frac{25}{24})^{1/2}$	$\langle\nu^c\rangle=0$
$\langle\tilde{n}\rangle=\chi_2$	1	1	0	$(\frac{10}{9})^{1/2}$	0	$\langle N\rangle=x$

$$\chi_1=\langle N^c\rangle\neq 0,\quad \chi_2=\langle n\rangle\neq 0\ .$$

An argument has recently been presented that while $\chi_2\lesssim 1$ TeV, χ_1 must be zero or vanishingly small.[16] In a rank-5 scenario $\chi_1\neq 0$ results in a broken global symmetry leading to a Goldstone boson (a_N) coupled to the divergence of the $B-L$ current. Further, $\chi_1\neq 0$ also leads to a mixing between the h quark ($-\frac{1}{3}$ charge isosinglet of the 27 representation) and the d quark through a term in the superpotential of the type (allowed by E_6 invariance)

$$\lambda_{ijk}d_i^c h_j N_k^c\ ,$$

where i, j, and k refer to generation indices. This coupling causes flavor-changing currents to raise in the neutral-current sector, and results in $K^+\to\pi^+ a_N$ decay. Present bounds on the absence of this decay lead to a limit $\chi_1<40$ keV. This argument implies that $\chi_1\approx 0$ in the rank-5 scenario and $\chi_2\neq 0$ then breaks the group to the standard model. On the other hand, in a rank-6 scenario, $\chi_1\neq 0$ does not lead to a Goldstone boson because the additional gauge boson absorbs this degree of freedom in becoming massive through the Higgs mechanism. Nevertheless an argument has been advanced that the field N^c still does not develop a VEV in the rank-6 scenario but for a different reason. Since there is no linear term in the field N^c in the superpotential arising from 27^3 terms, in order to develop VEV the potential should contain a mass term for $\tilde{N}^c$ with $m_{N^c}{}^2<0$. Such a term can be induced from renormalization-group scaling from a Yukawa coupling provided its strength exceeds the $U(1)_{B-L}$ gauge coupling which tends to drive the mass in the opposite direction. The only Yukawa terms in the superpotential involving N^c are

$$g_{ijk}L_i^{(2)}L_j^{(1)}N_k^c+\lambda_{ijk}h_k d_j^c N_k^c\ ,$$

where $L_2=(\nu_E,E)$ doublet and $L_1=(\nu_e,e)$ doublet. Then g_{ijk} is expected to be quite small ($g\sim 10^{-9}$), for this term gives Dirac mass to the neutrinos. The term $\lambda_{ijk}\langle N_k^c\rangle$ causes mixings between h_i and d_j quarks. This mixing leads to an off-diagonal quark coupling to Z (and other neutral gauge bosons) and is constrained by experiments. The present bounds which arise mostly from the K system are most restrictive for the first generation and imply λ's involving light quarks $\lesssim\frac{1}{25}$. However, such mixing constraints are weak for heavy-quark sectors, where $\lambda\approx 1$ can easily be tolerated. It is not unusual for Yukawa couplings to show intergenerational differences, as, for example, those causing the difference between quark masses. Thus we can assume that $\chi_1\neq 0$ can be driven by a sufficiently strong Yukawa coupling. Another possibility is for N^c to couple to 27's from $(27,\overline{27})$ multiplets. There are no restrictions on these couplings. Unless one assumes that all λ's are of the same magnitude, there is no compelling phenomenological reason to exclude a rank-6 group. In our discussion we shall assume that the χ_i are arbitrary but less than about 1 TeV.

III. MASS MATRIX AND LAGRANGIAN

The quantum numbers and VEV's for the neutral scalars in the 27 are listed in Table I. The resulting Z-boson mass-squared matrix in the Z,Z_ψ,Z_χ basis is

$$\mathcal{M}_Z{}^2=g_Z{}^2\begin{bmatrix} A & \sqrt{x_W}B & \sqrt{x_W}D \\ \sqrt{x_W}B & x_W C & x_W E \\ \sqrt{x_W}D & x_W E & x_W F \end{bmatrix}\ , \tag{1}$$

where for the 27 representation

$$\begin{aligned} A&=\tfrac{1}{2}(v_1{}^2+v_2{}^2+v_3{}^2)\equiv\tfrac{1}{2}v^2\ ,\\ B&=(\tfrac{5}{72})^{1/2}(2v_1{}^2-2v_2{}^2+v_3{}^2)\ ,\\ C&=\tfrac{5}{36}(4v_1{}^2+4v_2{}^2+v_3{}^2+\chi_1{}^2+16\chi_2{}^2)\ ,\\ D&=\frac{1}{\sqrt{24}}(2v_1{}^2+2v_2{}^2-3v_3{}^2)\ ,\\ E&=\tfrac{1}{12}(\tfrac{5}{3})^{1/2}(4v_1{}^2-4v_2{}^2-3v_3{}^2+5\chi_1{}^2)\ ,\\ F&=\tfrac{1}{12}(4v_1{}^2+4v_2{}^2+9v_3{}^2+25\chi_1{}^2)\ . \end{aligned} \tag{2}$$

Here $g_Z=e/[x_W(1-x_W)]^{1/2}$ and $x_W=\sin^2\theta_W$. In our calculations we will assume $x_W=0.23$. Equation (1) assumes that the evolution of all U(1) couplings from the grand unification scale to M_W is the same up to normalization constants. In the limit of one charged W boson at the electroweak scale

$$A=\left[\frac{8G_F}{\sqrt{2}}\right]^{-1}=\frac{M_Z{}^2}{g_Z{}^2}\ , \tag{3}$$

where M_Z is the standard-model Z mass. The neutral-current Lagrangian is

$$\mathcal{L}_{\rm NC}=g_Z(j_Z^\mu Z_\mu+\sqrt{x_W}j_\psi^\mu Z_{\psi\mu}+\sqrt{x_W}j_\chi^\mu Z_{\chi\mu}) , \quad (4)$$

where $j_A^\mu=\overline{\psi_L}Q_A\gamma_\mu\psi_L$ with $A=Z,\psi,\chi$. For the Z current, $Q_Z=I_{3L}-x_WQ$. The Q_ψ and Q_χ for neutral leptons are given in Table I; for the electron the values are $Q_\psi(e)=Q_\psi(e^c)=(\frac{5}{72})^{1/2}$, $Q_\chi(e)=-(\frac{3}{8})^{1/2}$, and $Q_\chi(e^c)=(\frac{1}{24})^{1/2}$. The Q values for quarks can be found in Ref. 8. The effective low-energy neutral-current Lagrangian is

$$\mathcal{L}_{\rm NC}^{\rm eff}=\frac{4G_F}{\sqrt{2}}(\rho_1 j_Z{}^2+\rho_2 j_\psi{}^2+\rho_3 j_\chi{}^2+\eta_1 j_Z j_\psi +\eta_2 j_Z j_\chi+\eta_3 j_\psi j_\chi) , \quad (5)$$

where

$$\begin{aligned}&\rho_1=A(CF-E^2)/H,\quad \eta_1=A(DE-BF)/H ,\\ &\rho_2=A(AF-D^2)/H,\quad \eta_2=A(BE-CD)/H ,\\ &\rho_3=A(AC-B^2)/H,\quad \eta_3=A(BD-AE)/H ,\\ &H=ACF-AE^2+2BDE-CD^2-B^2F .\end{aligned} \quad (6)$$

From Eqs. (2) and (3) we see that the v_i, which come from $SU(2)_L$ doublets, are constrained by the usual electroweak symmetry-breaking scale; the χ_i, which come from $SU(2)_L$ singlets, are not. We will examine the four possible cases whether the χ_i are large with respect to v, or not; for our purposes large χ_i means that the v_i may be ignored in the Z_2-Z_3 sector.

As we will see below, the extra Z bosons must be heavier than the Z_1, which is predominantly made up of the standard Z. This at least requires that the diagonal elements x_WC and x_WF in Eq. (1) be greater than A. Then from Eq. (2) it can be deduced that if the χ_i are not large, they must at least satisfy $\chi_i \gtrsim v$.

In the following we will use the convenient notation

$$\begin{aligned}&|Z(\alpha)\rangle=\cos\alpha\,|Z_\psi\rangle+\sin\alpha\,|Z_\chi\rangle ,\\ &|Z'(\alpha)\rangle=-\sin\alpha\,|Z_\psi\rangle+\cos\alpha\,|Z_\chi\rangle ,\end{aligned} \quad (7)$$

for the two linearly independent extra Z bosons, and will denote the mass eigenstates as Z_1,Z_2,Z_3.

IV. Z-BOSON SCENARIOS

Case 1. χ_1 and χ_2 large. In this case the standard Z essentially does not mix with the extra Z bosons; $Z_1=Z$. The remaining mass eigenstates are $Z_2=Z(\alpha)$ and $Z_3=Z'(\alpha)$ with

$$\tan2\alpha=\sqrt{15}/(8\chi_2{}^2/\chi_1{}^2-7) . \quad (8)$$

The Z_2,Z_3 masses are

$$M_{Z_{2,3}}{}^2=\tfrac{20}{9}x_WM_Z{}^2\times\{\chi_1{}^2+\chi_2{}^2\mp[(\chi_1{}^2-\chi_2{}^2)^2+\chi_1{}^2\chi_2{}^2/4]^{1/2}\}/v^2 . \quad (9)$$

The relation of M_{Z_2}/M_{Z_3} to the angle α is

$$\left[\frac{M_{Z_2}}{M_{Z_3}}\right]^2=\left[\frac{\cos\alpha+\sqrt{15}\sin\alpha}{\sqrt{15}\cos\alpha-\sin\alpha}\right]\left[\frac{\cos\alpha}{\sin\alpha}\right] . \quad (10)$$

By defining $M_{Z_2}<M_{Z_3}$ as above, it can be shown that the allowed range for α is restricted to

$$-\sqrt{15}/4\le\cos\alpha\le 0 . \quad (11)$$

Figure 1 shows M_{Z_2}/M_{Z_3} vs $\cos\alpha$. The maximum value of $(\frac{3}{5})^{1/2}$ occurs at $\cos\alpha=-(\frac{3}{8})^{1/2}$, so that Z_2 and Z_3 cannot be degenerate in mass in this scenario. Note that the lower-mass state Z_2 can never be the same as the rank-5 Z_2 for which $\cos\alpha=(\frac{5}{8})^{1/2}$. If we require that $\chi_i{}^2\ge 25v^2$ for this approximation to be good, we find $M_{Z_2}\ge 400$ GeV. The low-energy parameters are $\rho_1\simeq 1$; $\rho_2,\rho_3,\eta_1,\eta_2,\eta_3\ll 1$, so that the low-energy effective Lagrangian is nearly the same as the standard one.

Case 2. χ_1 large. In this case $Z_3=Z'(\alpha)$ with $\cos\alpha=-\sqrt{15}/4$ in Eq. (7). The Z_3 is much heavier than Z_1,Z_2 with mass

$$M_{Z_3}=(40x_W/9)^{1/2}(\chi_1/v)M_Z$$

and does not mix. The remaining extra Z boson $Z(\alpha)$ may mix with the standard Z:

$$\begin{aligned}&|Z_1\rangle=\cos\theta\,|Z\rangle+\sin\theta\,|Z(\alpha)\rangle ,\\ &|Z_2\rangle=-\sin\theta\,|Z\rangle+\cos\theta\,|Z(\alpha)\rangle ,\end{aligned} \quad (12)$$

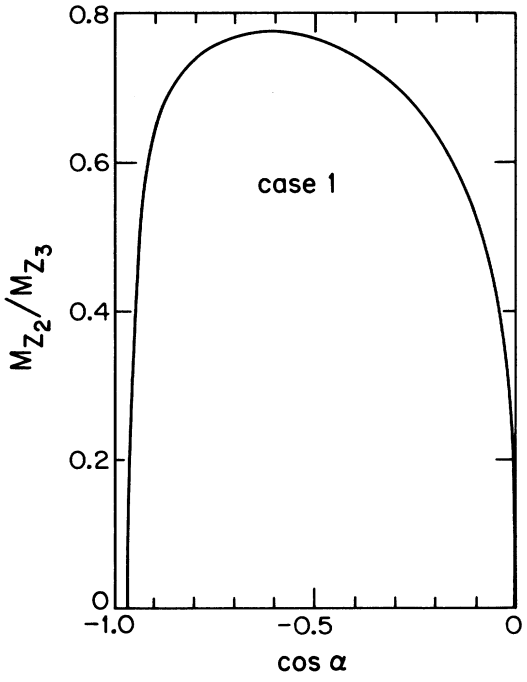

FIG. 1. The ratio M_{Z_2}/M_{Z_3} vs $\cos\alpha$ when both singlet VEV's are large (case 1).

and the Z_1, Z_2 masses are determined by

$$M_{Z_1}^2+M_{Z_2}^2=M_Z^2[1+x_W(4+5v_2^2/v^2+25\chi_2^2/v^2)/6] , \tag{13}$$

$$M_{Z_1}^2M_{Z_2}^2=M_Z^4 25x_W[v_2^2(1-v_2^2/v^2)/v^2+\chi_2^2/v^2]/6 .$$

There are two free parameters in the Z_1-Z_2 sector which we take to be M_{Z_2} and θ; M_{Z_1} is related to M_{Z_2} and θ by

$$\tan^2\theta=(M_{Z_1}^2-M_Z^2)/(M_Z^2-M_{Z_2}^2) . \tag{14}$$

The condition that M_{Z_1} must be close to the standard Z mass M_Z, as required by direct measurements at the CERN $p\bar{p}$ collider,[17] is depicted in Fig. 2(a). The allowed region in M_{Z_2}-θ parameter space is shown for various values of M_{Z_1}. We note that $M_{Z_1}\le M_Z$ for $M_{Z_2}\ge M_Z$, with the limit $M_{Z_1}\to M_Z$ occurring for $\theta\to 0$ (which does not necessarily require $M_{Z_2}\to\infty$). Also shown in Fig. 2(a) are the constraints from the Higgs structure, which are derived in the Appendix, and the limits from a 90%-C.L. fit to low-energy neutral-current data. The fitting procedure has been described before;[4] we varied the two parameters M_{Z_2} and θ with $x_W=0.23$ fixed. The low-energy parameters in this approximation are

$$\begin{aligned}
&\rho_1=M_Z^2(M_{Z_1}^2+M_{Z_2}^2-M_Z^2)/(M_{Z_1}^2M_{Z_2}^2) ,\\
&\rho_2=15\rho_3=-\sqrt{15}\eta_3=x_WM_Z^4/(16M_{Z_1}^2M_{Z_2}^2) ,\\
&\eta_1=-\sqrt{15}\eta_2\\
&\quad=(15x_W)^{1/2}\tan 2\theta M_Z^2\\
&\qquad\times(M_{Z_1}^2+M_{Z_2}^2-2M_Z^2)/(8M_{Z_1}^2M_{Z_2}^2) .
\end{aligned} \tag{15}$$

Case 3. χ_2 large. This is very similar to case 2, except that $\cos\alpha=0$ and the replacements $v_2\leftrightarrow v_3$, $\chi_1\leftrightarrow\chi_2$, and $\theta\to-\theta$ must be made in Eqs. (12)–(14). The allowed regions in M_{Z_2}-θ parameter space are shown in Fig. 2(b).

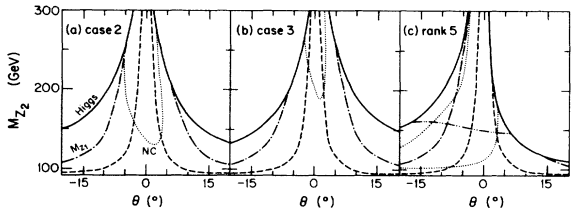

FIG. 2. Allowed regions in M_{Z_2}-θ parameter space for models for Z-$Z(\alpha)$ mixing: (a) $\cos\alpha=-\sqrt{15}/4$ (case 2), (b) $\cos\alpha=0$ (case 3), (c) $\cos\alpha=\sqrt{5/8}$ (rank 5), assuming $x_W=0.23$. The constraints are a 27 representation for the Higgs bosons (below solid curves), a two-parameter (M_{Z_2},θ) 90%-C.L. fit to low-energy neutral-current data (inside dotted region), the closeness of the Z_1 to the standard-model value, with $M_{Z_1}=0.98M_Z$ (below dash-dotted curves) and $M_{Z_1}=0.998M_Z$ (below dashed curves), and the limit from Z searches at the CERN $p\bar{p}$ collider with only the usual fermions contributing to Z_2 decay (above dash-dot-dot curve).

The low-energy parameters are

$$\begin{aligned}
&\rho_1=M_Z^2(M_{Z_1}^2+M_{Z_2}^2-M_Z^2)/(M_{Z_1}^2M_{Z_2}^2) ,\\
&\rho_3=x_WM_Z^4/(M_{Z_1}^2M_{Z_2}^2) ,\\
&\eta_2=\sqrt{x_W}\tan 2\theta M_Z^2\\
&\qquad\times(M_{Z_1}^2+M_{Z_2}^2-2M_Z^2)/(2M_{Z_1}^2M_{Z_2}^2) ,\\
&\rho_2,\eta_1,\eta_3\ll 1 ,
\end{aligned} \tag{16}$$

which can be obtained from Eq. (15) by rotating α from $\cos\alpha=-\sqrt{15}/4$ to $\cos\alpha=0$.

Case 4. Neither χ_1 nor χ_2 large. In this case all the VEV's may be of comparable size and no Z boson is extremely heavy; considerable mixing is possible. On the other hand, if the standard Z mixes appreciably with the other Z bosons then it will be shifted away from its standard mass value unless the masses are approximately degenerate. Although an extra Z boson with a mass near the standard Z mass is not ruled out by the search at the CERN $p\bar{p}$ collider—its branching ratio to lepton pairs could be suppressed by decays to exotic fermions—the lower limit on $Z(\alpha)$ or $Z'(\alpha)$ is roughly 150 GeV when the extra Z decays primarily into known fermions.[4,8] For simplicity we will examine the situation in the limit of no mixing between the Z and extra Z bosons. In this limit $B\to 0$, $D\to 0$, which implies $v_2^2=v_3^2=2v_1^2=2v^2/5$ and $Z_1=Z$. The extra Z bosons are $Z_2=Z(\alpha)$ and $Z_3=Z'(\alpha)$ as given by Eq. (7) with

$$\tan 2\alpha=\frac{\sqrt{15}(5\chi_1^2/v^2-2)}{40\chi_2^2/v^2-35\chi_1^2/v^2-2} \tag{17}$$

and the Z_2, Z_3 masses are determined by

$$\begin{aligned}
&M_{Z_2}^2+M_{Z_3}^2=\tfrac{8}{9}x_WM_Z^2(2+5\chi_1^2/v^2+5\chi_2^2/v^2) ,\\
&M_{Z_2}^2M_{Z_3}^2=\tfrac{4}{27}x_W^2M_Z^4(4+30\chi_1^2/v^2+30\chi_2^2/v^2\\
&\qquad+125\chi_1^2\chi_2^2/v^4) .
\end{aligned} \tag{18}$$

Contours of M_{Z_3} are shown in Fig. 3 versus M_{Z_2} and $\cos\alpha$ assuming $M_{Z_2}<M_{Z_3}$, as well as constraints from neutral-current data and Z searches. If we require $M_{Z_2}>M_Z$, as suggested by Z searches at the CERN $p\bar{p}$ collider, it is not hard to show that α is constrained to lie in the same range as case 1 [Eq. (11)]. Numerical studies of the mass matrix defined by Eqs. (1) and (2) show that if M_{Z_1} is constrained to be close to M_Z and $M_{Z_2}>150$ GeV, then Z mixing is small. Thus we feel that the no-mixing limit properly exemplifies this class of models.

Case 5. Rank 5. For E_6 breaking to a rank-5 group, the particular combination of $U(1)_\psi$ and $U(1)_\chi$ which becomes the extra U(1) is uniquely determined with $\cos\alpha=(\frac{5}{8})^{1/2}$ in Eq. (7). The extra Z boson $Z(\alpha)$ may mix with the standard Z [Eq. (12)] with the Z-$Z(\alpha)$ mixing angle θ given by Eq. (14). The mass matrix has been given before in the literature;[4,5] the allowed M_{Z_2}-θ parameter space is given in Fig. 2(c). If the Z_2 becomes heavy (≥ 400 GeV), Z-$Z(\alpha)$ mixing becomes negligible.

Comparing with Eq. (11) we see that in the limit that at

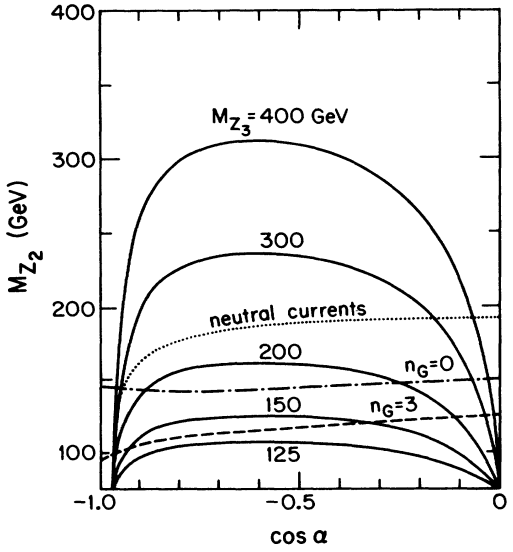

FIG. 3. Contours of Z_3 mass vs M_{Z_2} and cosα when neither χ_1 or χ_2 is large and the standard Z does not mix (case 4). Also shown are bounds on M_{Z_2} from low-energy neutral-current data (above dotted curve), and from Z_2 searches at the CERN $p\bar{p}$ collider with no ($n_G=0$) or all ($n_G=3$) exotic fermions contributing to Z_2 decay (above dash-dotted, dashed curves, respectively).

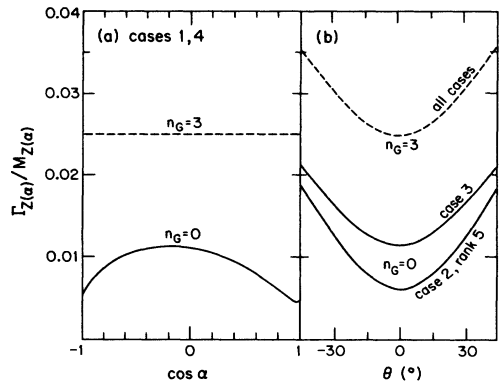

FIG. 4. Total decay width of Z_2 boson (a) without Z-$Z(\alpha)$ mixing (cases 1 and 4) and (b) with Z-$Z(\alpha)$ mixing (cases 2 and 3, rank 5).

least one χ_i is large, the rank-5 and rank-6 scenarios are distinct. Thus when E_6 is broken at the electroweak scale by the 27, if at least one extra Z is significantly heavier than the standard Z ($M_{Z_3} \geq 400$ GeV), then the rank-5 scenario may be distinguished from the various rank-6 scenarios by its couplings to fermions, which depend on α. We now examine this in detail. The analysis is somewhat different depending on whether one of the extra Z bosons mixes with the standard Z.

V. ANALYSIS

A. No Z-$Z(\alpha)$ mixing (cases 1, 4, and rank-5 scenario)

Nothing can be learned from the Z_1, since it is the standard one, so we turn to direct production of the extra Z's. The total decay rate of $Z(\alpha)$ as a function of α is given in Fig. 4; the decay branching fractions can be found in Ref. 8. In all discussions in this section, predictions for $Z'(\alpha)$ can be found from those for the $Z(\alpha)$ by the transformation $\alpha \rightarrow \alpha \pm \pi/2$.

Heavy extra Z bosons in cases 1 and 5 are unlikely to be produced below Superconducting SuperCollider (SSC) energies since $M_{Z_2}, M_{Z_3} \geq 400$ GeV. In Fig. 5 we show the total cross section and lepton pair signal for $pp \rightarrow Z(\alpha)X$ at $\sqrt{s}=40$ TeV vs cosα for a $Z(\alpha)$ with masses of 400 and 800 GeV. Case 1 is restricted to the region $-\sqrt{15}/4 \leq \cos\alpha \leq 0$, whereas a heavy $Z(\alpha)$ in the rank-5 scenario has $\cos\alpha = (\frac{5}{8})^{1/2}$.

In Case 4 $M_{Z_2}, M_{Z_3} \leq 400$ GeV but there are constraints from low-energy neutral-current data and Z-boson searches at the CERN $p\bar{p}$ collider.[17] Case 4 restrictions on α are the same as for case 1 for $M_{Z_2} > M_Z$. Measurements off the Z_1 resonance may also be useful for placing restrictions on a Z_2 which is not too heavy.[5,9,10,12,13] Predictions for the total cross section and lepton-pair signal for $p\bar{p} \rightarrow Z(\alpha)X$ at $\sqrt{s}=2$ TeV as a function of α have been given in Ref. 8.

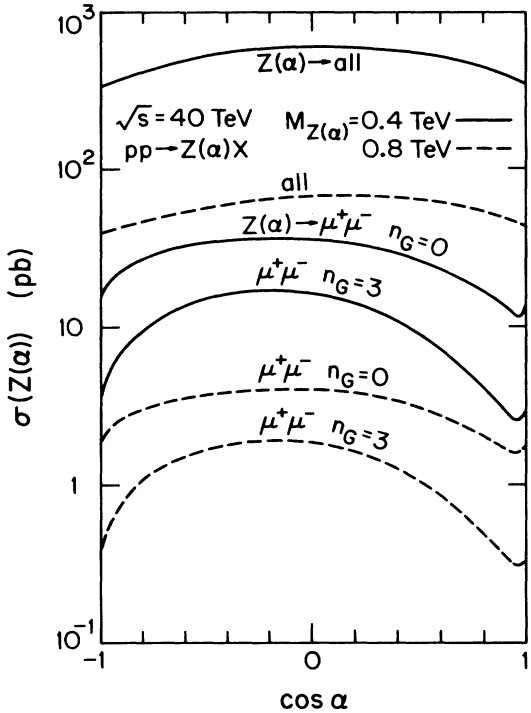

FIG. 5. Predictions for $Z_2 = Z(\alpha)$ production in a pp collider at $\sqrt{s}=40$ TeV shown vs cosα in case 1 for $M_{Z_2}=400$ and 800 GeV. Predictions for $Z_3 = Z'(\alpha)$ production are obtained by the transformation $\alpha \rightarrow \alpha \pm \pi/2$.

B. Z-$Z(\alpha)$ mixing (cases 2, 3, and rank-5 scenario)

The free parameters in these scenarios are M_{Z_2} and θ (we take $x_W=0.23$). For the rank-5 scenario, the limits from Z searches at the CERN $p\bar{p}$ collider are important, but only if one assumes the Z_2 decays exclusively into the usual fermions. Figure 6 shows the predicted Z_2 branching fractions vs θ. Because the Z mixes in this scenario, there are also constraints from direct studies of the Z_1 as well. Figure 7 shows the predicted cross section at $\sqrt{s}=630$ GeV vs θ for $p\bar{p}\to Z_1X$ with $Z_1\to e^+e^-$ decay; the 1σ allowed range from UA1 (Ref. 17) is shown for comparison. The current limits on θ from all constraints are approximately $-6°<\theta<4°$ (case 2), $-3°<\theta<3°$ (case 3), and $-20°<\theta<4°$ (rank 5).

Future precise studies of the Z_1 at Stanford Linear Collider (SLC) and CERN LEP can further restrict the parameters. Figure 8 gives the Z_1 fermion branching fractions vs θ. Figure 9 gives the production rate and polarization asymmetry in $e^+e^-\to\mu^+\mu^-$ on the Z_1 resonance versus θ. The production rate $R_{\mu\mu}$ integrated over the Z_1 resonance is

$$R_{\mu\mu}=\frac{\sigma(e^+e^-\to Z_1\to\mu^+\mu^-)}{\sigma(e^+e^-\to\gamma^*\to\mu^+\mu^-)_{\rm QED}}$$
$$=\frac{9\pi}{2\alpha^2}B(Z_1\to\mu^+\mu^-)^2 \tag{19}$$

and the polarization asymmetry on the Z_1 resonance is

$$A_{\rm pol}=\frac{\sigma_R-\sigma_L}{\sigma_R+\sigma_L}=\frac{2v_ea_e}{v_e^2+a_e^2}\ , \tag{20}$$

where v_e,a_e are the vector and axial-vector couplings of the electron to the Z_1, given by

$$v_e=(-\tfrac{1}{4}+x_W)\cos\theta+\tfrac{1}{2}[Q_\alpha(e)-Q_\alpha(e^c)]\sin\theta\ ,$$
$$a_e=\tfrac{1}{4}\cos\theta+\tfrac{1}{2}[-Q_\alpha(e)-Q_\alpha(e^c)]\sin\theta\ . \tag{21}$$

Here $Q_\alpha=Q_\psi\cos\alpha+Q_\chi\sin\alpha$. In Fig. 10 we show v_e and a_e for the models with Z-$Z(\alpha)$ mixing, along with limits from $e^+e^-\to l^+l^-$ at SLAC PEP and DESY PETRA (Ref. 18). Figure 11 shows the downward shift in the mass of the lowest Z resonance from the standard-model value as a result of Z-$Z(\alpha)$ mixing. Off-resonance measurements may also yield information on a Z_2 which is not too heavy. In Fig. 12 we show the total cross section

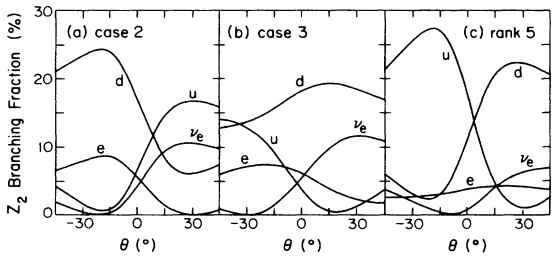

FIG. 6. Branching ratios of Z_2 boson with no exotic fermions contributing to Z_2 decay ($n_G=0$): (a) case 2, (b) case 3, and (c) rank 5.

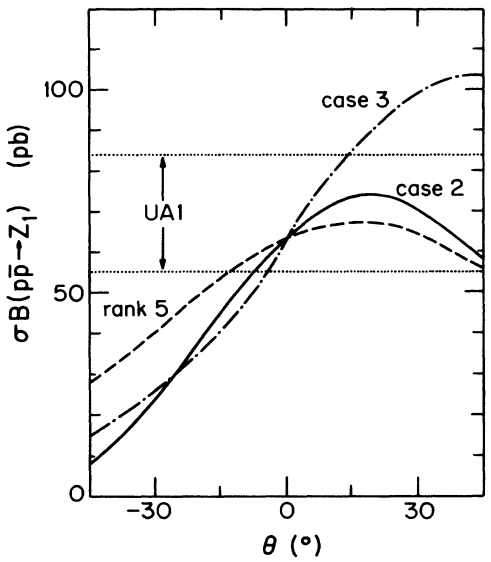

FIG. 7. Z_1 production cross section times e^+e^- branching ratio vs Z-$Z(\alpha)$ mixing angle θ at $\sqrt{s}=630$ GeV for case 2 (solid curve), case 3 (dash-dotted), rank-5 scenario (dashed), and the 1σ limits measured at UA1 (dotted).

and lepton-pair signal for $p\bar{p}\to Z(\alpha)X$ at $\sqrt{s}=2$ TeV vs θ for various M_{Z_2} values for the cases with Z-$Z(\alpha)$ mixing.

With a mass above 400 GeV, the Z_3 has the same properties as the $Z'(\alpha)$ of case 1 in the limits $\cos\alpha=-\sqrt{15}/4$ (case 2) and $\cos\alpha=0$ (case 3), and would probably not be seen before SSC. The rank-5 case has no Z_3.

VI. SUMMARY

We now summarize the results when E_6 is broken by the 27 representation. If no extra Z boson has a mass below about 400 GeV, then both singlet VEV's are large and the Z_1 should behave like the standard-model Z. Evidence for these heavy Z bosons would probably first come at a machine such as SSC; they would have different

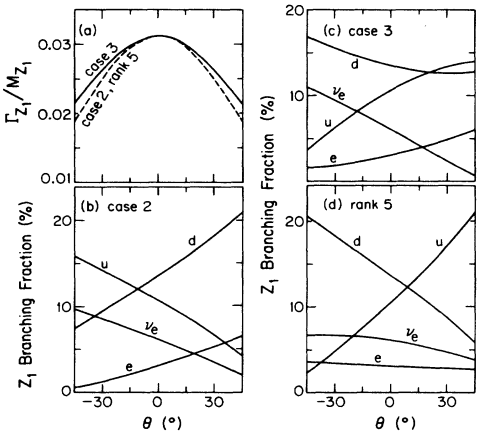

FIG. 8. (a) Total width of Z_1 in models with Z-$Z(\alpha)$ mixing; Z_1 branching ratios vs Z-$Z(\alpha)$ mixing angle θ for (b) case 2, (c) case 3, and (d) rank-5 case.

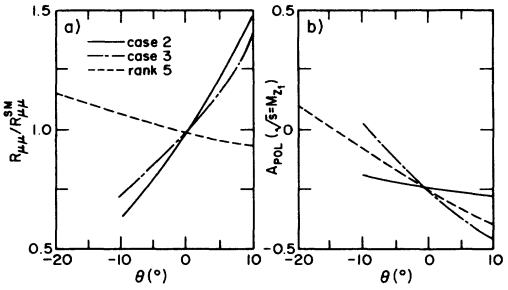

FIG. 9. (a) Relative production rate $R_{\mu\mu}/R_{\mu\mu}^{SM}$ and (b) polarization asymmetry A_{pol} on Z_1 resonance vs Z-$Z(\alpha)$ mixing angle θ.

properties in the rank-6 scenario than they would for rank-5 breaking. If exactly one extra Z boson has a mass below 400 GeV, then only particular linear combinations of $U(1)_\psi$ and $U(1)_\chi$ are allowed for the extra U(1) involved. There are two possibilities from rank-6 breaking of E_6 and one from rank-5 breaking. These different models may be distinguished from each other by the properties of the extra Z itself, or from its mixing with the standard Z,which may be determined by a detailed examination of the Z_1. If there are two extra Z bosons with mass below 400 GeV, then there is more freedom in the parameters; however, in the limit that the standard Z does not mix, the couplings of the extra Z's are somewhat constrained.

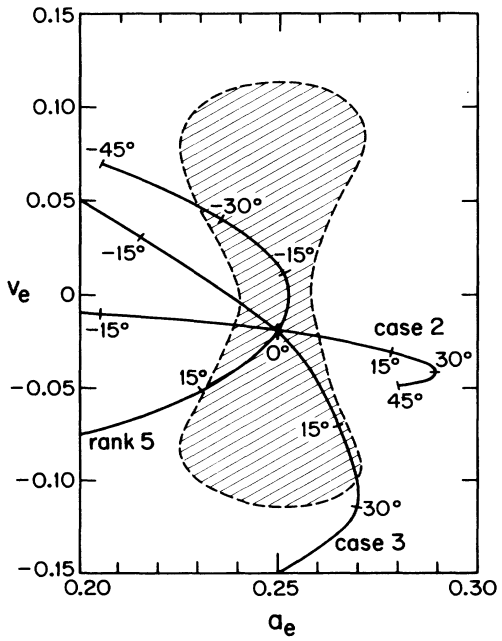

FIG. 10. Vector and axial-vector couplings of the electron to the Z_1 boson in models with Z-$Z(\alpha)$ mixing. The curves show the variation with the mixing angle for three different models. The shaded area represents the allowed region at 2σ C.L. from e^+e^- data (see Ref. 18).

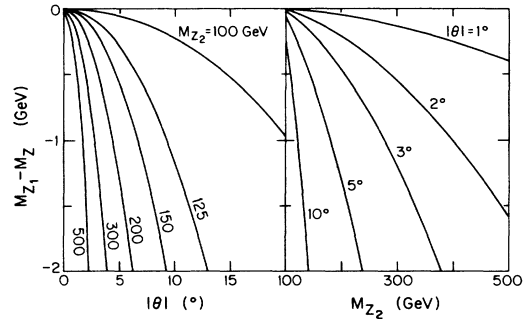

FIG. 11. Shift in the lower Z-boson mass value from its standard model value due to Z-$Z(\alpha)$ mixing with angle θ.

APPENDIX

In this appendix we briefly discuss the procedure for deriving limits on the Z boson masses and mixing for two Z bosons, given the Higgs structure of a 2×2 Z-boson-mass-squared matrix. If the mass-squared matrix has the form

$$\mathcal{M}_Z{}^2 = M_Z{}^2 \begin{bmatrix} a & b \\ b & c \end{bmatrix} \tag{A1}$$

in the Z-$Z(\alpha)$ basis, then the rotation to a diagonal basis Z_1-Z_2,

$$\begin{bmatrix} Z \\ Z(\alpha) \end{bmatrix} = \begin{bmatrix} \cos\theta & -\sin\theta \\ \sin\theta & \cos\theta \end{bmatrix} \begin{bmatrix} Z_1 \\ Z_2 \end{bmatrix}, \tag{A2}$$

leads to the conditions

$$a = (M_{Z_1}{}^2\cos^2\theta + M_{Z_2}{}^2\sin^2\theta)/M_Z{}^2 , \tag{A3a}$$

$$b = (M_{Z_2}{}^2 - M_{Z_1}{}^2)\sin\theta\cos\theta/M_Z{}^2 , \tag{A3b}$$

$$c = (M_{Z_1}{}^2\sin^2\theta + M_{Z_2}{}^2\cos^2\theta)/M_Z{}^2 . \tag{A3c}$$

In cases 2 and 3 and for rank-5 breaking $a=1$ and Eq. (A3a) gives

$$M_{Z_1}{}^2 = M_Z{}^2 + \tan^2\theta(M_Z{}^2 - M_{Z_2}{}^2) . \tag{A4}$$

The limits in M_{Z_2}-θ parameter space from the proximity of the Z_1 mass to the standard Z mass are easily ob-

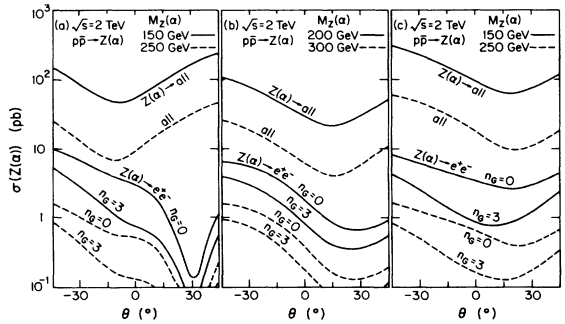

FIG. 12. Predictions for Z_2 production in $p\bar{p}$ collider at $\sqrt{s}=2$ TeV for various Z_2 mass values shown vs Z-$Z(\alpha)$ mixing angle θ: (a) case 2, (b) case 3, and (c) rank-5 scenario.

tained.

Also using $a=1$ we find

$$b=\tan\theta(M_Z{}^2-M_{Z_2}{}^2)/M_Z{}^2 , \tag{A5a}$$

$$c=[M_Z{}^2\tan^2\theta+M_{Z_2}{}^2(1-\tan^2\theta)]/M_Z{}^2 . \tag{A5b}$$

Constraints on b and c from the Higgs structure can now be imposed. For instance, in case 2,

$$b=\sqrt{x_W/6}(5v_2{}^2/v^2-2) , \tag{A6}$$

where $0\le v_2{}^2\le v^2$. If we choose $-\pi/4\le\theta\le\pi/4$ (so that the Z is predominantly made up of the Z_1), then Eqs. (A5a) and (A6) imply

$$\begin{aligned} -\sqrt{3x_W/2}\cot\theta &\le M_{Z_2}{}^2/M_Z{}^2-1 \\ &\le\sqrt{2x_W/3}\cot\theta \quad \text{for } 0\le\theta\le\pi/4 , \\ -\sqrt{2x_W/3}\,|\cot\theta| &\le M_{Z_2}{}^2/M_Z{}^2-1 \\ &\le\sqrt{3x_W/2}\,|\cot\theta| \quad \text{for } -\pi/4\le\theta\le 0 . \end{aligned} \tag{A7}$$

The constraint from c is not as strong. For case 3, b has the opposite sign from Eq. (A6) and therefore the allowed regions are the mirror image in θ from those in Eq. (A7).

In the rank-5 scenario

$$b=\sqrt{x_W}(5v_1{}^2/v^2-1)/3 \tag{A8}$$

for which the restriction $0\le v_1{}^2\le v^2$ gives

$$\begin{aligned} -4\sqrt{x_W}\cot\theta/3 &\le M_{Z_2}{}^2/M_Z{}^2-1 \\ &\le\sqrt{x_W}\cot\theta/3 \quad \text{for } 0\le\theta\le\pi/4 , \\ -\sqrt{x_W}\,|\cot\theta|/3 &\le M_{Z_2}{}^2/M_Z{}^2-1 \\ &\le 4\sqrt{x_W}\,|\cot\theta|/3 \quad \text{for } -\pi/4\le\theta\le 0 . \end{aligned} \tag{A9}$$

[1]M. B. Green and J. H. Schwarz, Phys. Lett. **149B**, 117 (1984); **151B**, 21 (1985).

[2]P. Candelas, G. Horowitz, A. Strominger, and E. Witten, Nucl. Phys. **B258**, 46 (1985); E. Witten, *ibid.* **B258**, 75 (1985); M. Dine, V. Kaplunovsky, M. Mangano, C. Nappi, and N. Seiberg, *ibid.* **B259**, 549 (1985).

[3]See, e.g., J. L. Rosner, Comments Nucl. Part. Phys. **15**, 195 (1986); P. Binetruy *et al.*, Nucl. Phys. **B273**, 501 (1986); R. W. Robinett, Phys. Rev. D **26**, 2388 (1982).

[4]V. Barger, N. G. Deshpande, and K. Whisnant, Phys. Rev. Lett. **56**, 30 (1986).

[5]J. Ellis *et al.*, Nucl. Phys. **B276**, 14 (1986); Mod. Phys. Lett. **A1**, 57 (1986); V. D. Angelopoulos *et al.*, Phys. Lett. **176B**, 203 (1986); E. Cohen *et al.*, *ibid.* **165B**, 76 (1985).

[6]S. M. Barr, Phys. Rev. Lett. **55**, 2778 (1985).

[7]L. S. Durkin and P. Langacker, Phys. Lett. **166B**, 436 (1986).

[8]V. Barger, N. G. Deshpande, J. L. Rosner, and K. Whisnant, Wisconsin Report No. MAD/PH/299 (unpublished).

[9]G. Belanger and S. Godfrey, TRIUMF Report No. TRI-PP-86-18, 1986 (unpublished); Phys. Rev. D **34**, 1309 (1986).

[10]David London and J. L. Rosner, Phys. Rev. D **34**, 1530 (1986); David London, G. Belanger, and J. N. Ng, TRIUMF Report No. TRI-PP-86-78, 1986 (unpublished).

[11]F. del Aguila *et al.*, CERN Report No. TH.4376/86, 1986 (unpublished).

[12]P. J. Franzini and F. J. Gilman, Phys. Rev. D **35**, 855 (1987).

[13]J. L. Hewett, T. G. Rizzo, and J. A. Robinson, Phys. Rev. D **33**, 1476 (1986); **34**, 2179 (1986); T. G. Rizzo, *ibid.* **34**, 2076 (1986); **34**, 2699 (1986).

[14]T. Matsuoka *et al.*, Nagoya University Reports Nos. DPNU-86-08, 1986, DPNU-86-09, 1986, and DPNU-86-10, 1986 (unpublished).

[15]A. Sen, Phys. Rev. Lett. **55**, 33 (1985).

[16]B. Campbell, J. Ellis, M. K. Gaillard, D. V. Nanopoulos, and K. A. Olive, Phys. Lett. **180B**, 77 (1986).

[17]UA1 Collaboration, S. Geer, Proceedings of the XXIII International Conference on High Energy Physics, Berkeley, California, 1986 (unpublished).

[18]B. Naroska, DESY Report No. 86-051 (unpublished).